Delay effects on the limit cycling behavior in an H-bridge resonant inverter with zero current switching control strategy

L. Benadero[a], F. Torres[b], A. El Aroudi[c], C. Olalla[c], E. Ponce [b] and L. Martinez-Salamero[c]

[a] Departament de Física, Universitat Politècnica de Catalunya, Barcelona, Spain
[b] Departamento de Matemática Aplicada, Escuela Técnica Superior de Ingeniería, Universidad de Sevilla, Sevilla, Spain
[c] Departament d'Enginyeria Electrònica, Elèctrica i Automàtica, Universitat Rovira i Virgili, Tarragona, Spain
luis@fa.upc.edu, ftorres@us.es, abdelali.elaroudi@urv.cat, carlos.olalla@urv.cat, eponcem@us.es, luis.martinez@urv.cat

Abstract—In this paper, bifurcations of limit cycles in a H-bridge LC resonant inverter under a zero current switching control strategy with delay in the switching action are analyzed. Mathematical analysis and numerical simulations show that the delay can degrade the quality of the oscillations and even inhibit them.

1. Introduction

Resonant inverters are systems in which oscillations in an LC tank circuit are sustained by means of a switching network, thus converting a DC voltage into an AC one. We consider here self-sustained oscillations that are produced by switching the active branch of the bridge whenever the current in the LC tank becomes zero [1, 2, 3]. This zero current switching (ZCS) control strategy has the advantage of minimizing switching losses. A generalized model of a resonant DC-AC H-bridge inverter, which includes the parallel and series implementations, was introduced and its bifurcation scenery was analyzed in [4], without considering the delay. Here, the delay effect on the limit cycling behavior is analyzed from the switched model, and the results are confirmed by direct simulations.

In Section 2, a normalized model of the inverter is introduced in the form of a delay differential system with only three parameters, and in Section 3, the bifurcation pattern is described highlighting the influence of the delay.

2. System description and mathematical modeling

The circuit diagram of the system under study is depicted in Fig. 1. It consists of a generalized circuit including parasitic resistances in the energy storage elements, which can represent both series and parallel topologies. The following elements can be identified: the input voltage V_g; the output series resistance R_{os}; the inductor with inductance L and parasitic series resistor r_{ls}; the output parallel conductance $G_{op} = 1/R_{op}$; the capacitor with capacitance C, parasitic parallel conductance $g_{cp} = 1/r_{cp}$ and parasitic series resistance r_{cs}; and the switches S_1, S_2, S_3 and S_4.

The circuit operation is based on an automatically activated switching between two configurations. The switches are driven by the two signals δ and its complementary

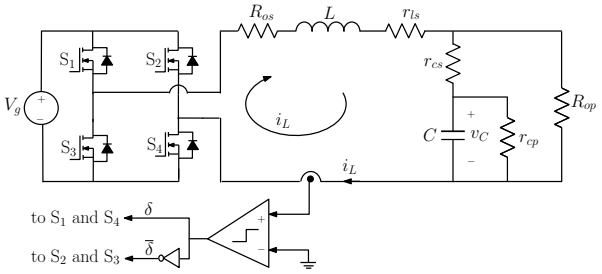

Figure 1: Generalized schematic diagram of an LC resonant inverter. Note that if a resistor is missing, either its corresponding conductance or resistance vanishes.

$\bar{\delta} = 1 - \delta$. Note that $\delta = 1$ when the inductor current $i_L > 0$ and $\delta = 0$ if $i_L < 0$, so that a ZCS control is implemented in a natural way. In that diagram, $\delta = 1\,(0)$ forces the ON (OFF) state in S_1 and S_4 and the OFF (ON) state in S_2 and S_3.

Note that if the switching is inhibited, the capacitor voltage and the inductor current tend to be constant; specifically, if $\delta = 1\,(0)$, there is an equilibrium point with positive (negative) capacitor voltage and inductor current. Otherwise, a limit cycle is possible when the switching is active. This oscillating regime is built by a suitable aggregation of two orbits, each one being a part of the transient regime toward one of the equilibrium pair. However, this desired objective is only achieved for certain values of the parameters and some initial conditions, as it is shown later.

First, a piecewise-linear model for the system shown in Fig. 1 will be obtained by ignoring the delay; for more details, see [4]. Let v_C be the capacitor voltage and i_L the inductor current. By applying KVL and KCL, one gets

$$uV_g = L\frac{\mathrm{d}i_L}{\mathrm{d}t} + i_L(R_{os} + r_{ls}) + i_{cs}r_{cs} + v_C,$$

$$i_L = i_{cs} + (i_{cs}r_{cs} + v_C)G_{op},$$

where i_{cs}, that is the current through r_{cs}, is

$$i_{cs} = C\frac{\mathrm{d}v_C}{\mathrm{d}t} + g_{cp}v_C.$$

The variable $u = 2\delta - 1$ is determined by the control, such that $u = 1\,(-1)$, that is $\delta = 1\,(0)$, if $i_L > 0\,(< 0)$.

After some algebra, the following model is obtained

$$\frac{\mathrm{d}}{\mathrm{d}t}\begin{pmatrix} v_C \\ i_L \end{pmatrix} = \mathbf{A}\begin{pmatrix} v_C \\ i_L \end{pmatrix} + u\mathbf{b}, \tag{1}$$

where

$$\mathbf{A} = \begin{pmatrix} -\frac{G_p}{C} & \frac{\kappa}{C} \\ -\frac{\kappa}{L} & -\frac{R_s}{L} \end{pmatrix}, \quad \mathbf{b} = \begin{pmatrix} 0 \\ \frac{V_g}{L} \end{pmatrix}, \tag{2}$$

and the factor κ, the equivalent series resistance R_s and the equivalent parallel conductance G_p are

$$\kappa = \frac{1}{1 + r_{cs}G_{op}}, \; R_s = R_{os} + r_{ls} + \kappa r_{cs}, \; G_p = g_{cp} + \kappa G_{op}.$$

Let $\det(\mathbf{A})$ and $\mathrm{tr}(\mathbf{A})$ be the determinant and trace of matrix $\mathbf{A}$ in (2). Hence, the natural frequency $\omega_0 = \sqrt{\det(\mathbf{A})}$ and the quality factor $Q = -\omega_0/\mathrm{tr}(\mathbf{A})$ of the LC tank are

$$\omega_0 = \sqrt{\frac{R_sG_p + \kappa^2}{LC}}, \quad \frac{1}{Q} = \frac{G_p}{\omega_0 C} + \frac{R_s}{\omega_0 L}.$$

Below, the model will be expressed in a canonical form with dimensionless parameters. Let β be a first normalized parameter defined as

$$\beta = \frac{QG_p}{\omega_0 C} = 1 - \frac{R_sQ}{\omega_0 L} = \frac{G_pL}{G_pL + CR_s}. \tag{3}$$

Note that $0 \leq \beta \leq 1$. The case $\beta = 0\,(1)$ arises when $G_p = 0\,(R_s = 0)$, that is the ideal series (parallel) inverter. Assuming $Q > 1/2$, the eigenvalues of matrix $\mathbf{A}$ are

$$p^{\pm} = -\frac{\omega_0}{2Q} \pm i\omega_0\sqrt{1 - \frac{1}{4Q^2}} = \omega_0(\sigma \pm i\nu), \tag{4}$$

in which $\sigma = -(2Q)^{-1}$ and $\nu = \sqrt{1 - (2Q)^{-2}}$. Let γ be a second normalized parameter, related to the relative energy losses of the LC tank, defined as

$$\gamma = \frac{\sigma}{\nu} = \frac{-1}{\sqrt{4Q^2 - 1}} < 0. \tag{5}$$

Now, by means of the following change of variables

$$\theta = \nu\omega_0 t, \quad \mathbf{x} = \begin{pmatrix} x_1 \\ x_2 \end{pmatrix} = \begin{pmatrix} \frac{\kappa}{V_g} & -\frac{LG_p}{CV_g} \\ 0 & \frac{\nu\omega_0 L}{V_g} \end{pmatrix}\begin{pmatrix} v_C \\ i_L \end{pmatrix}, \tag{6}$$

system (1) can be reformulated as

$$\frac{\mathrm{d}\mathbf{x}}{\mathrm{d}\theta} = \mathbf{A}\mathbf{x} + u\mathbf{b}, \tag{7}$$

where matrix $\mathbf{A}$ and vector $\mathbf{b}$ are redefined as

$$\mathbf{A} = \begin{pmatrix} 0 & 1 + \gamma^2 \\ -1 & 2\gamma \end{pmatrix}, \quad \mathbf{b} = \begin{pmatrix} 2\beta\gamma \\ 1 \end{pmatrix}. \tag{8}$$

Then, the new matrix $\mathbf{A}$ has the eigenvalues

$$\lambda^{\pm} = \gamma \pm i.$$

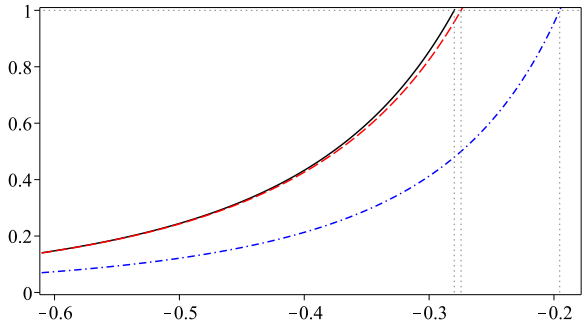

Figure 2: Plots of $\beta_{sn}(\gamma)$, $\beta_{cc}(\gamma)$ and $\beta_{hc}(\gamma)$, in solid black, dashed red and dash-dotted blue, respectively. The line $\beta = 1$ marks the maximum value for this parameter and vertical lines give account of the corresponding minimum values of parameter γ to avoid the homoclinic connection, critical crossing and fold bifurcation for any valid value of β.

Considering an ideal switching forced by the condition $i_L = 0$, the switching function, in accordance to the change of variables (6), is given by the expression $h(\mathbf{x}) = x_2$.

However, if a delayed switching action is considered, the control signal u is determined by a past state of the system. Let us consider, as an approximation to the problem, a fixed switching time delay T_d due to switches and driving circuitry. Then, the model of our system is the differential equation (7)-(8), together with the delayed switching function

$$h(\mathbf{x}, t) = h(\mathbf{x}(t - \tau)) = x_2(t - \tau), \tag{9}$$

where the normalized time delay $\tau = \nu\omega_0 T_d$ is a third parameter in addition to β and γ. Then, $u = 1$ if $h(\mathbf{x}(\mathbf{t} - \tau)) > 0$ and $u = 0$ if $h(\mathbf{x}(\mathbf{t} - \tau)) < 0$. Note that system (7)-(9) with a constant value $u = \pm 1$, has the following equilibria

$$\overline{\mathbf{x}}^{\pm} = (\overline{x}_1, \overline{x}_2)u = \pm\left(1 - \frac{4\beta\gamma^2}{1 + \gamma^2}, \frac{-2\beta\gamma}{1 + \gamma^2}\right), \tag{10}$$

which may be constant solutions of the switched system, whenever $\beta > 0$, since $\overline{x}_2 > 0$.

3. Crossing limit cycle and its bifurcations

Apart from the stable equilibria (10), the dynamics of system (7)-(9) can also be oscillatory. Without delay, the only possible stable oscillation is made up by two linked trajectories. However, with delay, more complex oscillations can occur. In the following, the conditions for existence of limit cycles without delay are revisited, and then, the case with delay is addressed.

3.1. Revisiting limit cycles existence without delay

Solutions for any of the two linear configurations in (7), starting at $\mathbf{x}(0)$, can be expressed as

$$\mathbf{x}(\theta) = \Phi^{\pm}(\theta, \mathbf{x}(0)) = \phi(\theta)\left(\mathbf{x}(0) - \overline{\mathbf{x}}^{\pm}\right) + \overline{\mathbf{x}}^{\pm}, \tag{11}$$

where $\phi(\theta)$ is the evolution operator given by

$$\phi(\theta) = e^{\gamma\theta}\begin{pmatrix} \cos\theta - \gamma\sin\theta & (1+\gamma^2)\sin\theta \\ -\sin\theta & \cos\theta + \gamma\sin\theta \end{pmatrix}.$$

Note that without delay, the configuration changes whenever the orbit crosses the switching manifold

$$\Sigma = \{\mathbf{x} = (x_1, 0), x_1 \in \mathbb{R}\}. \tag{12}$$

Furthermore, in the subset of the switching manifold $\Sigma^s = \{\mathbf{x} = (x_1, 0), -1 \le x_1 \le 1\}$, the escaping sliding conditions are satisfied, i.e., the vector field points outward both sides of Σ^s. Due to this property, the sliding subset Σ^s plays a relevant role in the existence of unstable sliding cycles. These cycles are boundaries between the region of attraction of the oscillatory dynamics and that of different equilibria.

A complete classification of limit cycle configurations for system (7-9), without delay and with parameter $\beta > 0$, appears in Theorem 1 in [4]. In such theorem, limit cycle conditions are summarized. For the sake of completeness, such conditions are reproduced below.

(a) If $0 < \beta < \beta_{hc}(\gamma)$ then there exist one stable crossing limit cycle and two unstable sliding limit cycles.

(b) If $\beta = \beta_{hc}(\gamma)$ then there exist one stable crossing limit cycle and two homoclinic connections to the origin.

(c) If $\beta_{hc}(\gamma) < \beta < \beta_{cc}(\gamma)$ then there exist one stable crossing limit cycle and one unstable sliding limit cycle.

(d) If $\beta = \beta_{cc}(\gamma)$ then there exist one stable crossing limit cycle and one unstable critical crossing limit cycle.

(e) If $\beta_{sn}(\gamma) < \beta < \beta_{cc}(\gamma)$ then there exist two crossing limit cycles having opposite stability.

(f) If $\beta = \beta_{sn}(\gamma)$ then there is one crossing limit cycle which is semi-stable.

(g) If $\beta > \beta_{sn}(\gamma)$ then there are no crossing limit cycles.

Consequently, four regions are found in the parameter plane (β, γ) defined by the three functions $\beta_{sn}(\gamma), \beta_{cc}(\gamma)$ and $\beta_{hc}(\gamma)$, which are codimension-one lines corresponding to a smooth fold, also called saddle-node, bifurcation of cycles, to a critical crossing-sliding cycle and to a double homoclinic saddle connection, respectively. These functions are depicted in Fig. 2, and some cases for limit sets are shown in Fig. 3.

3.2. Limit cycles bifurcations under delay action

Although the switching is theoretically induced at time instants such that the orbit crosses Σ, actually the transition between the two configurations is delayed due to the non ideal features of the switches. In Fig. 4(a), the stable limit cycle has been computed for three values of the delay, resulting in smaller cycles when the delay is increased, until this closed orbit collides with Σ for the highest value of τ.

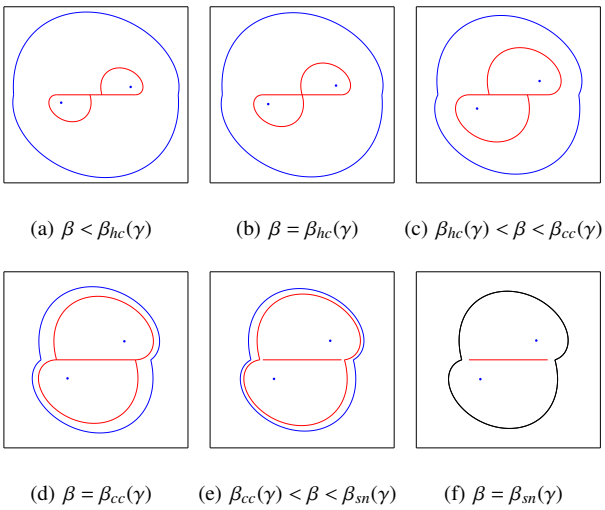

(a) $\beta < \beta_{hc}(\gamma)$ (b) $\beta = \beta_{hc}(\gamma)$ (c) $\beta_{hc}(\gamma) < \beta < \beta_{cc}(\gamma)$

(d) $\beta = \beta_{cc}(\gamma)$ (e) $\beta_{cc}(\gamma) < \beta < \beta_{sn}(\gamma)$ (f) $\beta = \beta_{sn}(\gamma)$

Figure 3: Limit sets for parameters $\tau = 0$, γ fixed and β given in the caption. The equilibrium points and the outer stable limit cycle are depicted in blue color and the unstable cycles in red color. The black cycle in (f) is the non hyperbolic limit cycle at the fold bifurcation. The red straight line corresponds to the sliding set Σ^s.

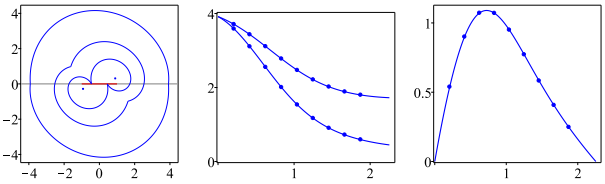

(a) (x_1, x_2) plane (b) $x_1^c, -x_1^s$ (τ) (c) x_2^s (τ)

Figure 4: (a) Limit cycles for $\tau \in \{0, 1, 2.252586...\}$. (b) Crossing and switching values of x_1 and (c) switching values of x_2, versus τ. Fixed parameters $\beta = 1, \gamma = -0.15$. Dots in (b-c) are from simulations in the steady state.

Let $\mathbf{x}^s = (x_1^s, x_2^s)$ be the point of the orbit at the actual switching instant, $\mathbf{x}^c = (x_1^c, 0)$ be the point where the orbit crosses Σ, and θ_s be the half-period of the cycle. Taking into account the vector field symmetry, limit cycles with delay can be obtained by solving the equation set

$$\Phi^+(\theta_s, \mathbf{x}^s) = -\mathbf{x}^s, \qquad \Phi^+(\theta_s - \tau, \mathbf{x}^s) = \mathbf{x}^c. \tag{13}$$

Note that the four algebraic equations in (13) must be solved for the set of four unknowns $\{\theta_s, x_1^s, x_2^s, x_1^c\}$.

In Fig. 4(b-c), x_1^c, $-x_1^s$ and x_2^s have been represented versus the delay τ. The curves have been computed from (13), and the dots have been obtained by long time running simulations. The fixed parameters β and γ used in the quoted figure are such that, when increasing τ, the standard limit cycle is annihilated by a border collision with the switching manifold Σ, as it can be appreciated in Fig. 4(a). This critical value of τ can be computed by forcing $x_2^s = 0$, taking τ as the forth unknown in (13). Notice that, in the border

collision condition, $\mathbf{x}^s \in \Sigma^s$.

There is, however, another possible bifurcation for the stable limit cycle, when delay is increased, which can be understood as an evolution of the smooth saddle-node bifurcation of cycles mentioned in the above section. In this case, for some critical values of the parameter set $\{\beta, \gamma, \tau\}$, a nonhyperbolic limit cycle exists, such that when decreasing τ, two crossing limit cycles, the outer stable and the inner unstable, are given. Simulations show that this bifurcation, including the switching delay, has the same qualitative features than the ideal case (without delay) analyzed in [4].

In Fig. 5(a-b), the two bifurcations for crossing limit cycles have been represented in the plane (γ, τ), with $\beta = 1$. The red (blue) line corresponds to the smooth (border-collision) case. Note the existence of a codimension-two bifurcation point for the intersection of those codimension-one lines. The critical values $\gamma_1 = -0.26239683$ and $\tau_1 = 0.48856227$ have been determined for this point for $\beta = 1$. Note also that if $\gamma > \gamma_1$ ($\gamma < \gamma_1$), the border collision takes place for the stable (unstable) crossing cycle.

Figure 5(c) is a diagram similar to that in Fig. 4(b), but with a more negative value of γ, in order to have a saddle-node bifurcation of cycles. In this diagram, blue (red) lines stand for stable (unstable) cycles. Here, the red line ends at a border collision of the unstable crossing cycle, similar the one explained above for the stable one.

3.3. Some estimation of a safe value for delay

The delay action introduces an important degree of complexity so that the determination of the boundary between the regions of attraction of the desired stable limit cycle and the equilibrium points is a difficult task. Although a formal analysis of this subject is out of the scope of this paper, we approach the problem by determining a critical value of the delay such that an orbit starting at the origin, $\mathbf{x}_0 = (0, 0)$, reaches the sliding subset of the switching manifold, Σ^s. This value is determined by the set of equations, with unknowns $\{\hat{\theta}, \hat{\tau}, \hat{x}_1^s, \hat{x}_1^c\}$,

$$\Phi^+(\hat{\theta}, \mathbf{x}_0) = \hat{\mathbf{x}}^s, \quad \Phi^+(\hat{\theta} - \hat{\tau}, \mathbf{x}_0) = \hat{\mathbf{x}}^c,$$

where $\hat{\tau}$ is the critical value of τ, $\hat{\theta}$ is the flight time from the origin to a point $\hat{\mathbf{x}}^s \in \Sigma^s$, with $0 < \hat{x}_1^s < 1$, and $\hat{\mathbf{x}}^c \in \Sigma$, is the crossing point of the orbit, with $\hat{x}_1^c > 1$.

The dashed green line in Fig. 5(a) corresponds to $\hat{\tau}(\gamma)$ with $\beta = 1$. Note that $\hat{\tau}\left(\beta_{hc}^{-1}(1)\right) = 0$. From this approach, we conclude that it is advisable a parameter set of the system below the dashed green line in Fig. 5(a) diagram, in order to guarantee the oscillatory dynamics under starting conditions near the origin of the phase state.

4. Conclusions

A smooth fold and a border collision bifurcations of cycles have been found for a H-bridge self resonant inverter if the switching delay is considered. The amplitude of the oscillation and some curves in the parameter space for these bifurcations have been computed.

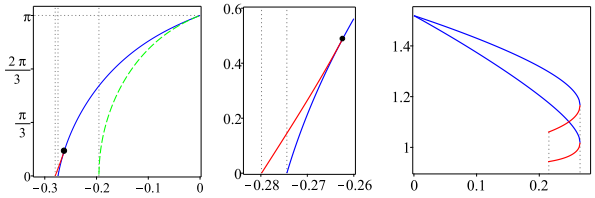

(a) $\tau(\gamma)$ (b) $\tau(\gamma)$ (c) $-x_1^c, -x_1^s\ (\tau)$

Figure 5: (a-b) Saddle-node in red color and border collision in blue color bifurcations of crossing limit cycles in the parameter plane (γ, τ) with fixed parameter $\beta = 1$, and (b) is a zoom. (c) Crossing and switching values of x_1 versus parameter τ in its valid interval, with fixed parameters $\beta = 1, \gamma = -0.27$; the values for the stable and for the unstable cycles are in blue and red colors respectively.

Acknowledgments

This work has been sponsored by the Spanish Agencia Estatal de Investigación (AEI) and the Fondo Europeo de Desarrollo Regional (FEDER) under grant DPI2017-84572-C2-1-R, by the Spanish Ministerio de Ciencia e Innovación under grant MTM2015-65608-P, and by the Consejería de Economía y Conocimiento de la Junta de Andalucía under grant P12-FQM-1658.

References

[1] C. S. Tang, Y. Sun, Y. G. Su, S. K. Nguang and A. P. Hu,"Determining multiple steady-state ZCS operating points of a switch-mode contactless power transfer system," *IEEE Transactions on Power Electronics*, vol. 24, no. 2, pp. 416–425, 2009.

[2] R. Bonache-Samaniego, C. Olalla and L. Martínez-Salamero, "Design of self-oscillating resonant converters based on a variable structure systems approach," *IET Power Electronics*, vol. 57, no. 1, pp. 111–119, 2015.

[3] R. Bonache-Samaniego, C. Olalla and L. Martínez-Salamero, "Dynamic Modeling and Control of Self-Oscillating Parallel Resonant Converters Based on a Variable Structure Systems Approach," *IEEE Transactions on Power Electronics*, vol. 32, no. 2, pp. 1469–1480, 2017.

[4] L. Benadero, E. Ponce, A. El Aroudi, F. Torres, "Limit cycle bifurcations in resonant LC power inverters under zero current switching strategy,", *Nonlinear Dynamics*, vol. 91, no. 2, pp. 1145–1161, 2018.